

Supporting Information

Anion Binding Consistency by influence of Aromatic *meta*- disubstitution of a Simple Urea Receptor: Regular Entrapment of Hydrated Halide and Oxyanion clusters

Utsab Manna, and Gopal Das*

Department of Chemistry, Indian Institute of Technology Guwahati, Assam-781039,

India

E-mail: gdas@iitg.ernet.in

Characterization of receptor L:

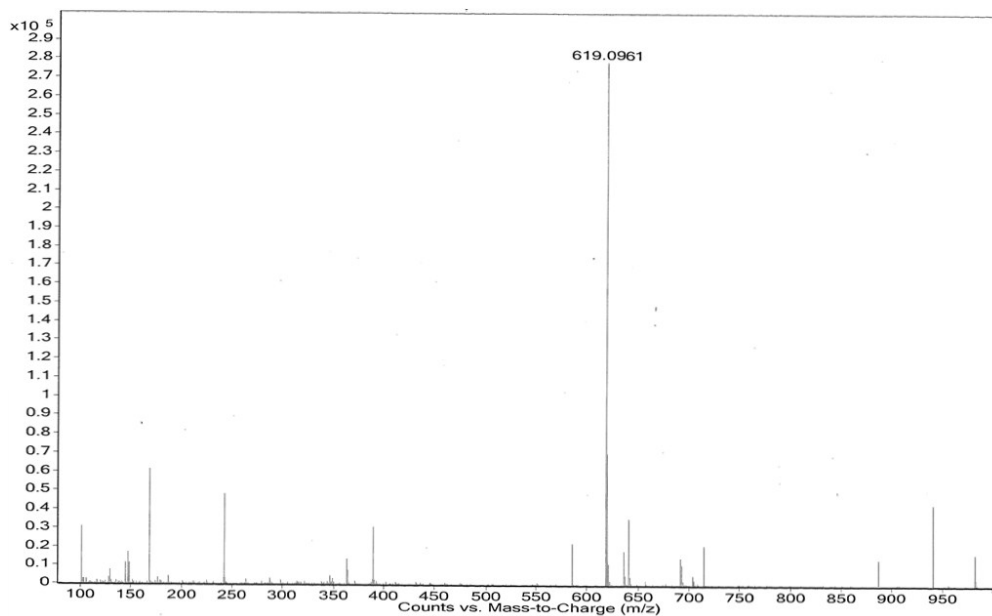


Figure S1: ESI-mass spectrum of receptor L.

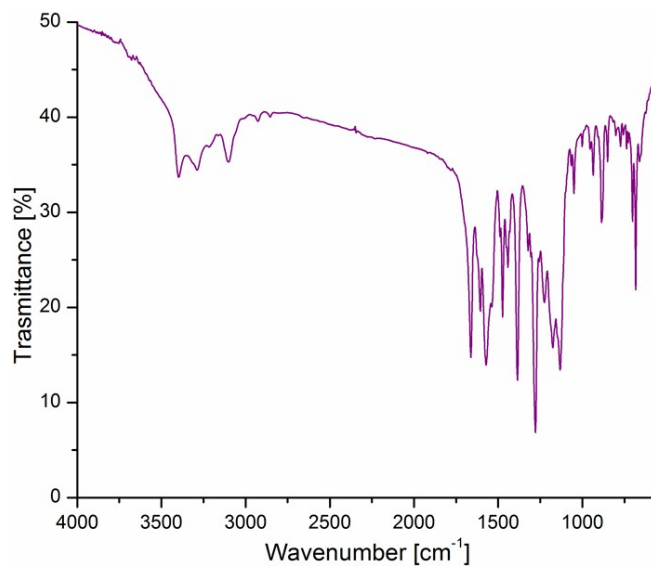


Figure S2: FT-IR spectrum of receptor L recorded in KBr pellet: 3199 cm⁻¹ ν s(N-H), 3289 cm⁻¹ ν s(C-H), 3096 cm⁻¹ ν s(C-H), 1641 cm⁻¹ ν s(C=O), 1258 cm⁻¹ ν s(C-F).

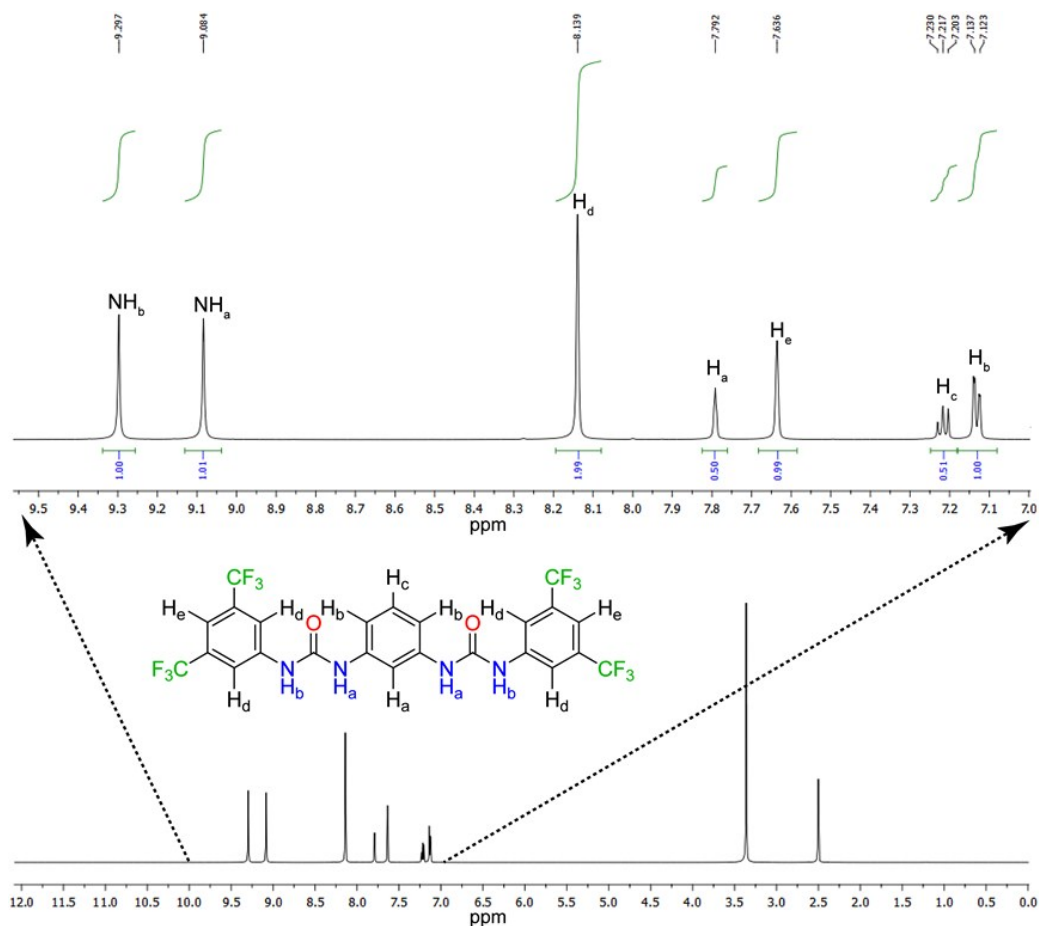


Figure S3: ^1H NMR spectrum of receptor **L** in $\text{DMSO-}d_6$ (600 MHz, $\text{DMSO-}d_6$) δ (ppm): 7.123-7.137 (d, 2H, ~ 8.4 Hz, Ar-H), 7.203-7.230 (t, 1H, ~ 7.8 Hz, Ar-H), 7.636 (s, 2H, Ar-H), 7.792 (s, 1H, Ar-H), 8.139 (s, 4H, Ar-H), 9.084 (s, 2H, NHa), 9.297 (s, 2H, NHb).

Characterization of complex **1**:

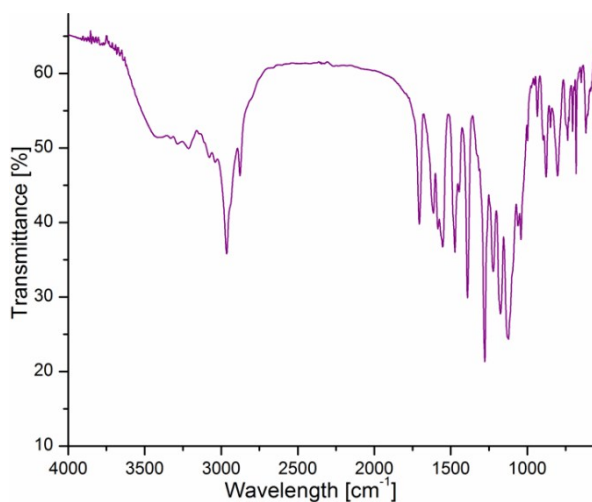


Figure S4: FT-IR spectrum of hydrated-sulphate complex **1** recorded in KBr pellet: broad band at 3425 cm^{-1} $\nu_s(\text{O-H})$, 3302 cm^{-1} $\nu_s(\text{N-H})$, 3218 cm^{-1} $\nu_s(\text{C-H})$, 2853 cm^{-1} $\nu_s(\text{C-H})$, 1678 cm^{-1} $\nu_s(\text{C=O})$, 1273 cm^{-1} $\nu_s(\text{C-F})$. 1198 cm^{-1} $\nu_s(\text{S-O})$.

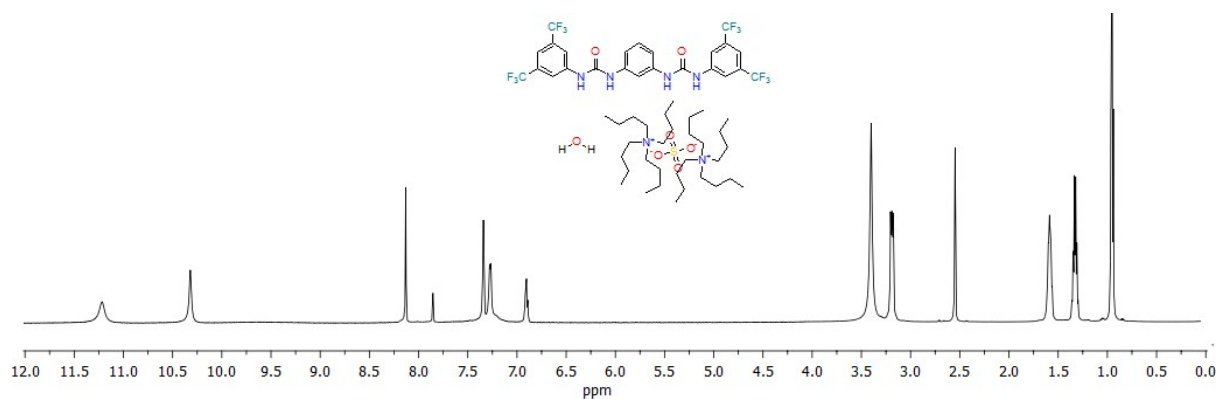


Figure S5: ^1H NMR spectrum of complex **1** in $\text{DMSO-}d_6$ (Varian-600 MHz) at 298 K, δ (ppm): 0.892-0.916 (t, 12H, ~ 7.2 Hz, TBA- CH_3), 1.251-1.311 (m, 8H, TBA- CH_2), 1.514-1.566 (m, 8H, TBA- CH_2), 3.128-3.156 (t, 8H, ~ 8.4 Hz, N^+ -TBA- CH_2), 6.890-6.917 (t, 1H, ~ 8.4 Hz, Ar-H), 7.267-7.278 (d, 2H, ~ 6.6 Hz, Ar-H), 7.341 (s, 2H, Ar-H), 7.816 (s, 1H, Ar-H), 8.129 (s, 4H, Ar-H), 10.320 (s, 2H, NH_a), 11.212 (s, 2H, NH_b).

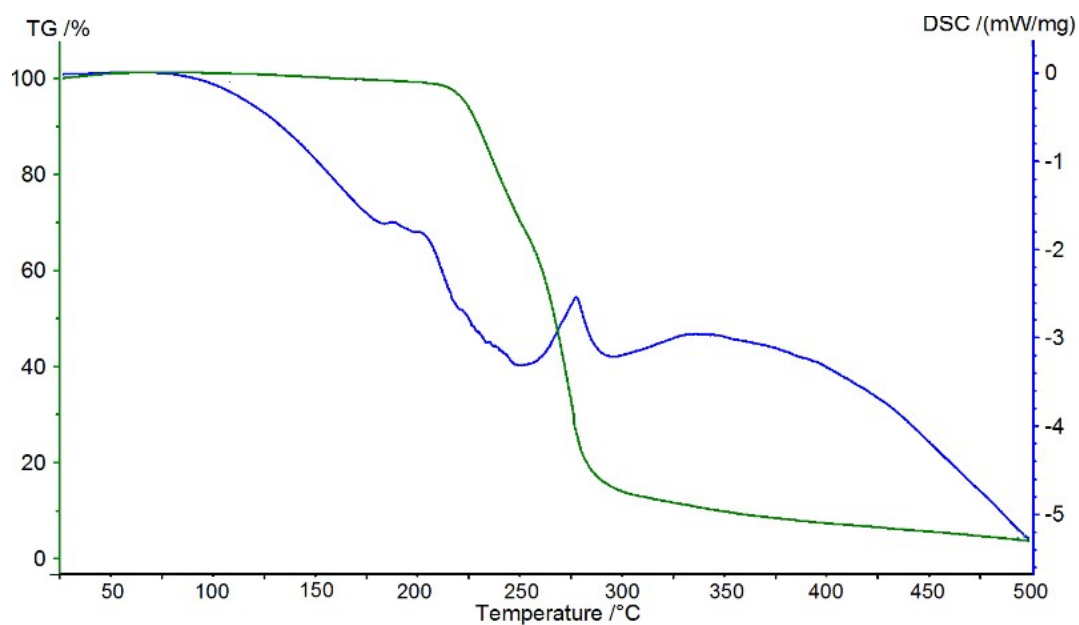


Figure S6: Thermogravimetric analysis (TGA) curve differential scanning calorimetry (DSC) curve of complex **1** at a heating rate of $10\text{ }^\circ\text{C}$ per min.

Characterization of complex 2:

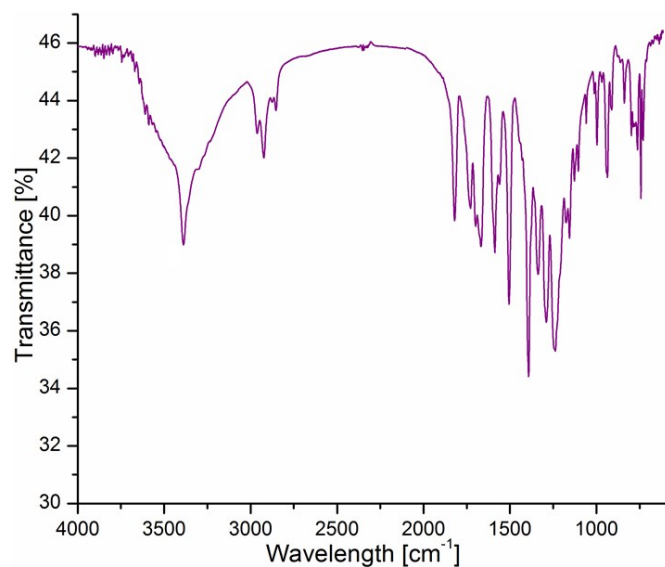


Figure S7: FT-IR spectrum of receptor bicarbonate-dimer complex **2** recorded in KBr pellet: 3258 cm^{-1} $\nu_s(\text{N-H})$, 3039 cm^{-1} $\nu_s(\text{C-H})$, 2876 cm^{-1} $\nu_s(\text{C-H})$, 1676 cm^{-1} $\nu_s(\text{C=O})$, 1257 cm^{-1} $\nu_s(\text{C-F})$.

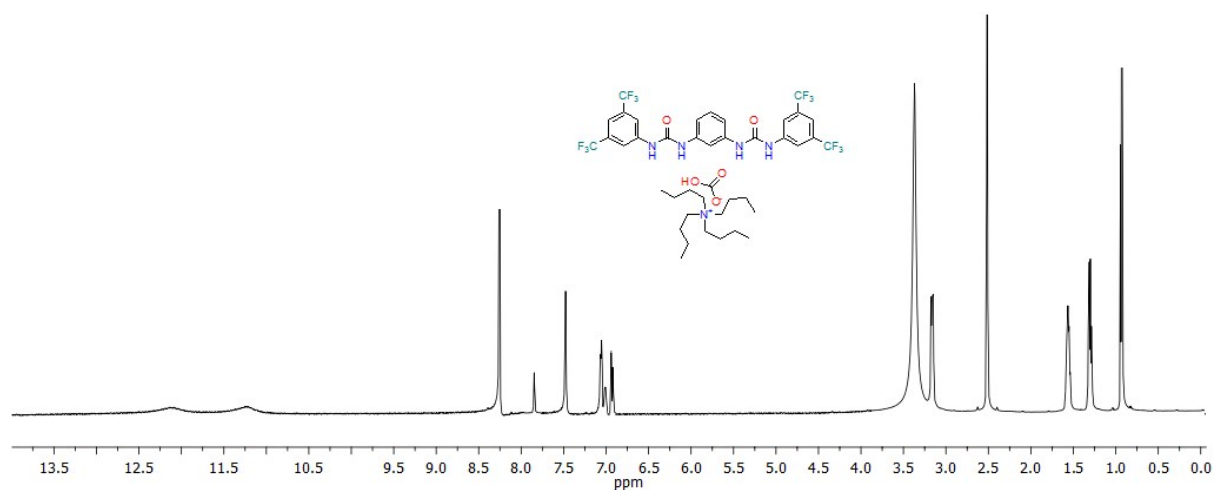


Figure S8: ^1H NMR spectrum of complex **2** in $\text{DMSO-}d_6$ (Varian-600 MHz) at 298 K, δ (ppm): 0.906-0.930 (t, 12H, ~ 7.2 Hz, TBA- CH_3), 1.261-1.323 (m, 8H, TBA- CH_2), 1.523-1.575 (m, 8H, TBA- CH_2), 3.134-3.162 (t, 8H, ~ 7.8 Hz, N^+ -TBA- CH_2), 6.923-7.107 (m, 3H, Ar-H), 7.477 (s, 2H, Ar-H), 7.865 (s, 1H, Ar-H), 8.254 (s, 4H, Ar-H), 11.221 (s, 2H, NH_a), 12.105 (s, 2H, NH_b).

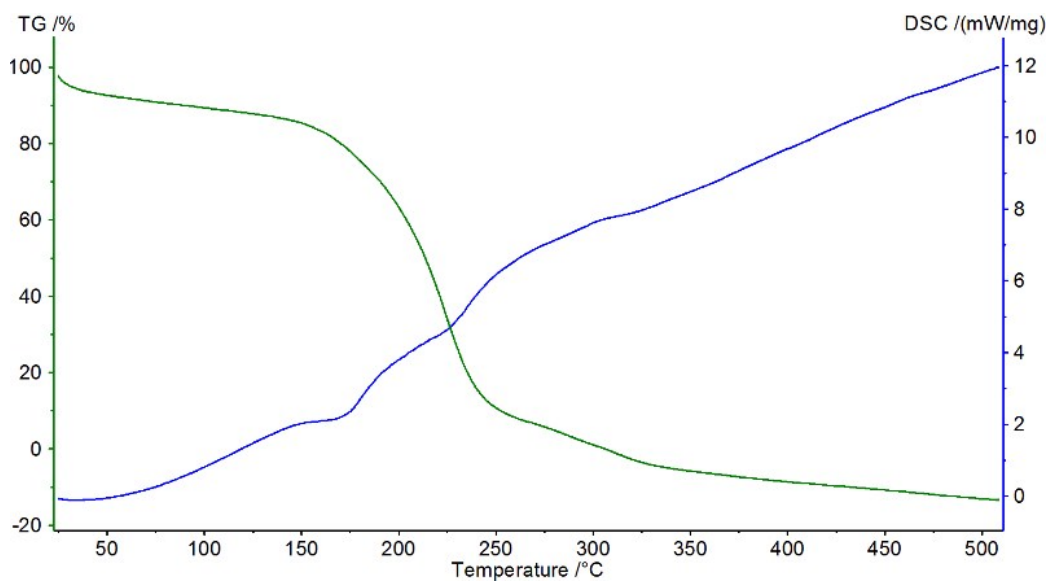


Figure S9: Thermogravimetric analysis (TGA) curve differential scanning calorimetry (DSC) curve of complex **2** at a heating rate of 10 °C per min.

Characterization of complex **3**:

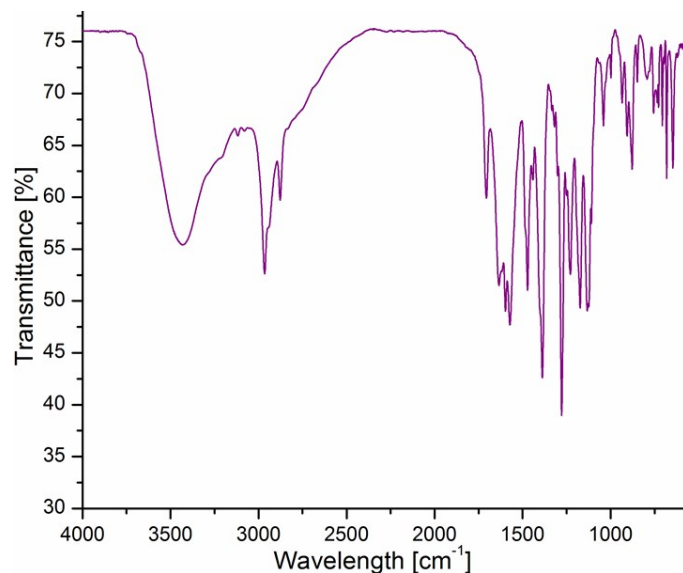


Figure S10: FT-IR spectrum of hydrated-acetate complex **3** recorded in KBr pellet: broad band at 3451 cm^{-1} $\nu_{\text{s}}(\text{O-H})$, 3345 cm^{-1} $\nu_{\text{s}}(\text{N-H})$, 3038 cm^{-1} $\nu_{\text{s}}(\text{C-H})$, 2836 cm^{-1} $\nu_{\text{s}}(\text{C-H})$, 1658 cm^{-1} $\nu_{\text{s}}(\text{C=O})$, 1265 cm^{-1} $\nu_{\text{s}}(\text{C-F})$.

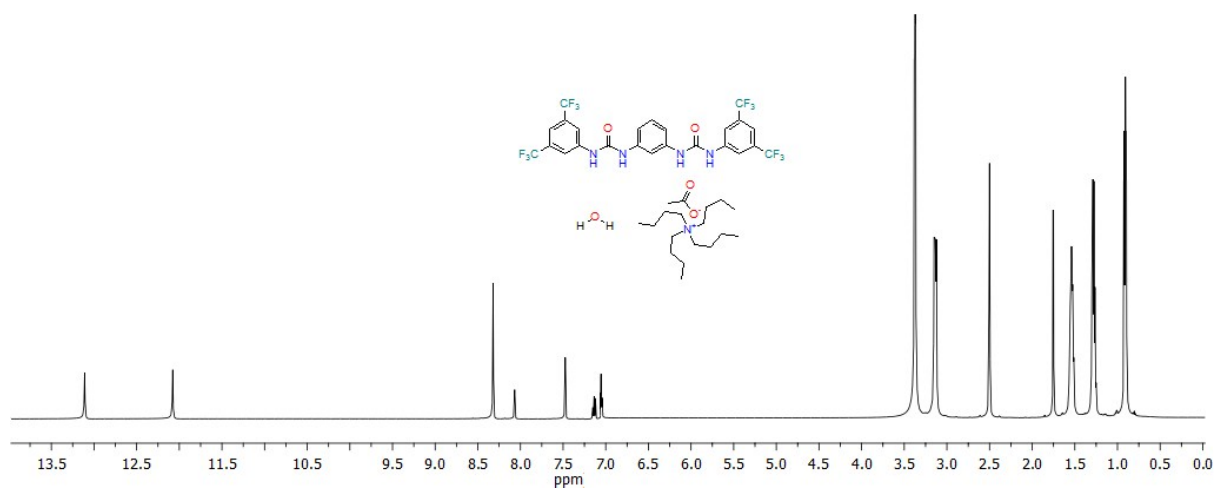


Figure S11: ^1H NMR spectrum of complex **3** in $\text{DMSO-}d_6$ (Varian-600 MHz) at 298 K, δ (ppm): 0.896-0.921 (t, 12H, ~ 7.8 Hz, TBA- CH_3), 1.251-1.312 (m, 8H, TBA- CH_2), 1.512-1.564 (m, 8H, TBA- CH_2), 1.752 (s, 3H, $-\text{CH}_3\text{COO}^-$), 3.122-3.150 (t, 8H, ~ 8.4 Hz, $\text{N}^+\text{-TBA-CH}_2$), 7.028-7.098 (m, 3H, Ar-H), 7.475 (s, 2H, Ar-H), 8.068 (s, 1H, Ar-H), 8.321 (s, 4H, Ar-H), 12.077 (s, 2H, NH_a), 13.110 (s, 2H, NH_b).

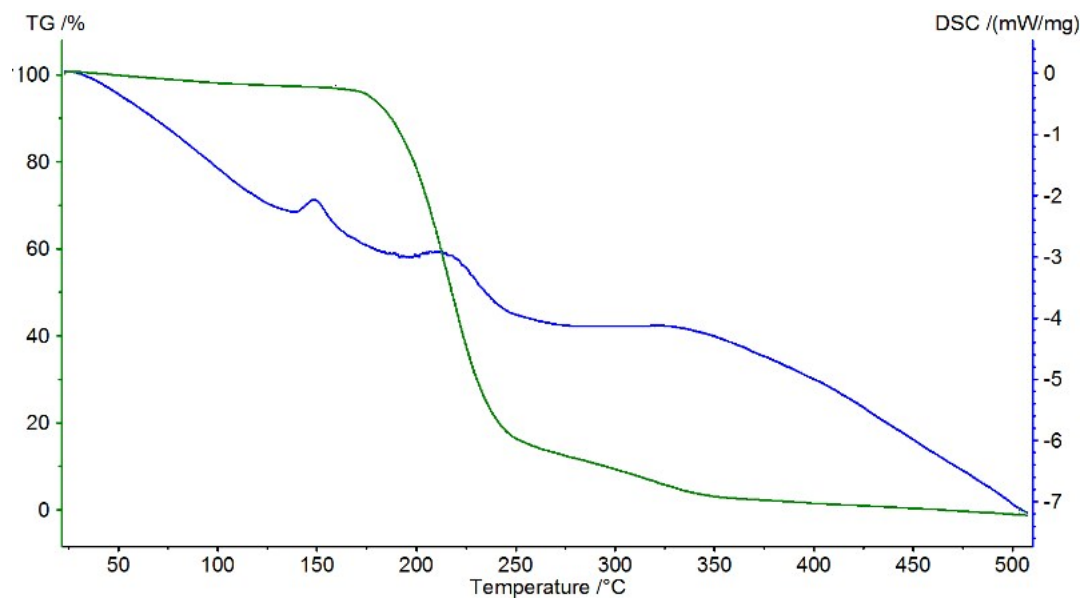


Figure S12: Thermogravimetric analysis (TGA) curve differential scanning calorimetry (DSC) curve of complex **3** at a heating rate of $10\text{ }^\circ\text{C}$ per min.

Characterization of complex 4:

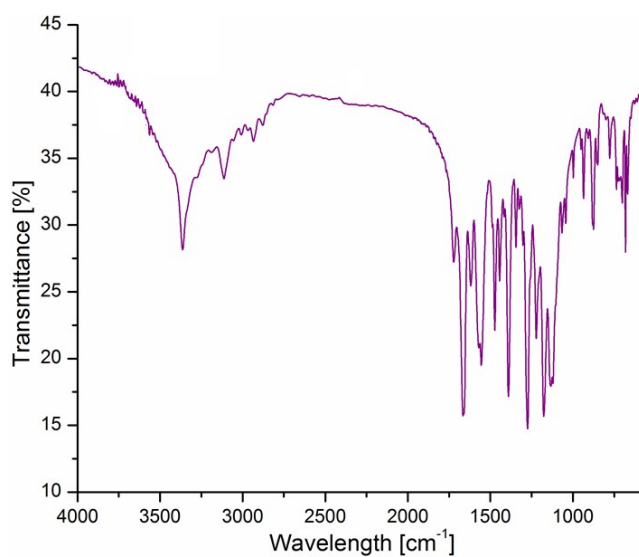


Figure S13: FT-IR spectrum of hydrated chloride complex **4** recorded in KBr pellet: 3373 cm^{-1} $\nu_s(\text{N-H})$, 3289 cm^{-1} $\nu_s(\text{C-H})$, 3108 cm^{-1} $\nu_s(\text{C-H})$, 1667 cm^{-1} $\nu_s(\text{C=O})$, 1261 cm^{-1} $\nu_s(\text{C-F})$.

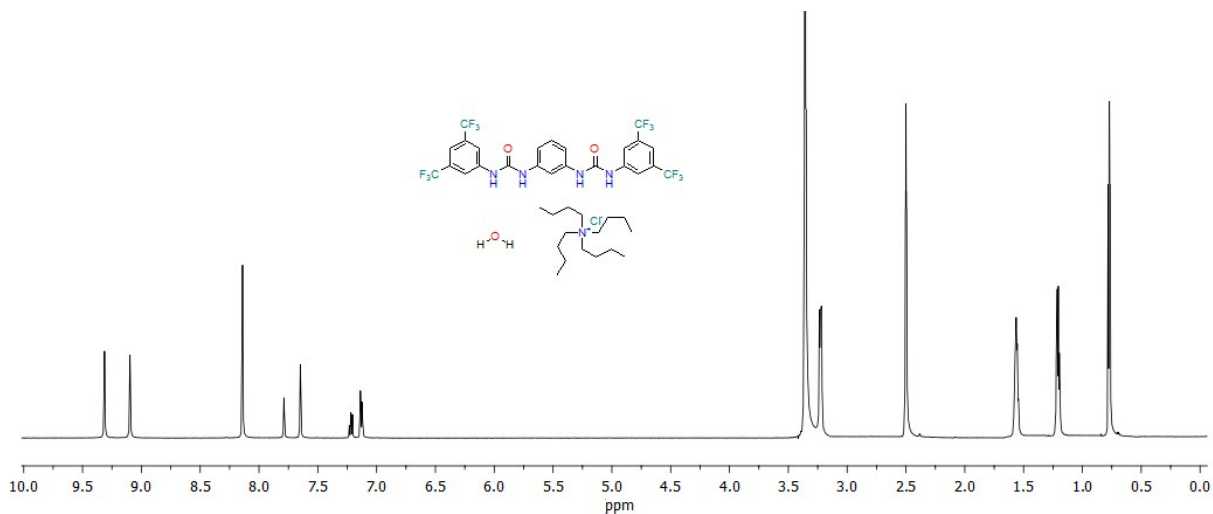


Figure S14: ^1H NMR spectrum of complex **4** in $\text{DMSO-}d_6$ (Varian-600 MHz) at 298 K, δ (ppm): 0.908-0.945 (t, 12H, ~ 7.2 Hz, TBA- CH_3), 1.254-1.347 (m, 8H, TBA- CH_2), 1.515-1.596 (m, 8H, TBA- CH_2), 3.137-3.179 (t, 8H, ~ 7.8 Hz, N^+ -TBA- CH_2), 7.121-7.135 (d, 2H, ~ 8.4 Hz, Ar-H), 7.205-7.232 (t, 1H, ~ 7.8 Hz, Ar-H), 7.648 (s, 2H, Ar-H), 7.788 (s, 1H, Ar-H), 8.140 (s, 4H, Ar-H), 9.097 (s, 2H, NH_a), 9.313 (s, 2H, NH_b).

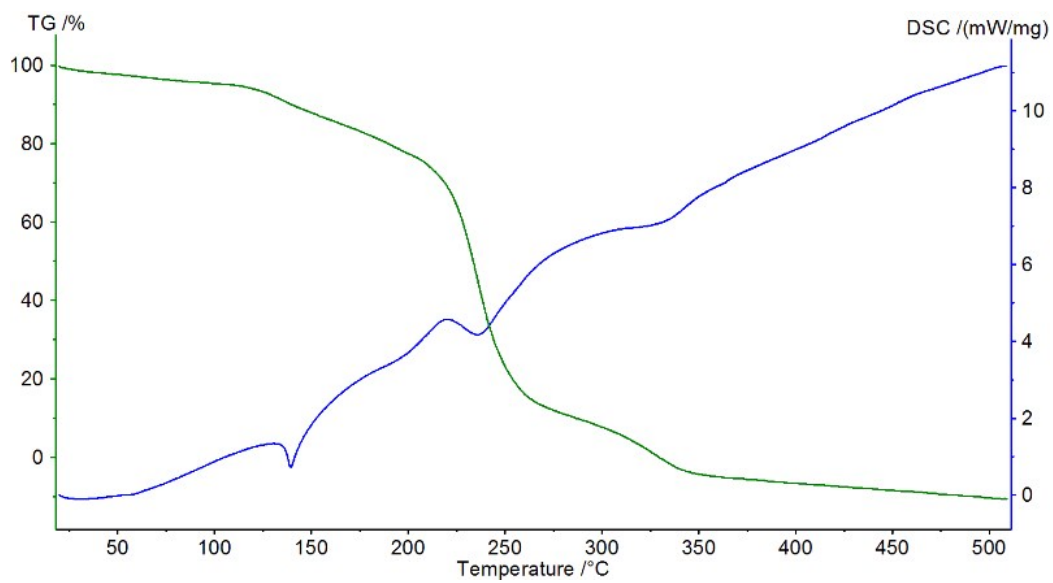


Figure S15: Thermogravimetric analysis (TGA) curve differential scanning calorimetry (DSC) curve of complex **4** at a heating rate of 10 °C per min.

Solution state anion binding study:

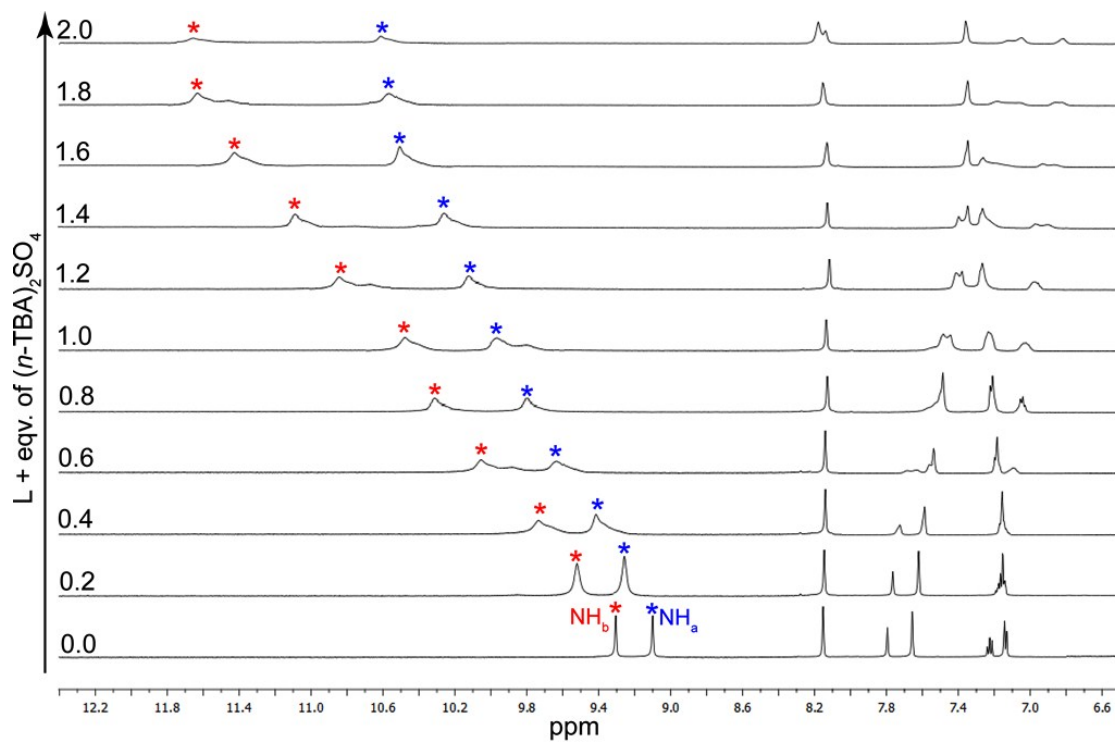


Figure S16: Expanded partial ^1H NMR spectra of **L** upon titration with $(n\text{-TBA})_2\text{SO}_4$ in DMSO-d_6 .

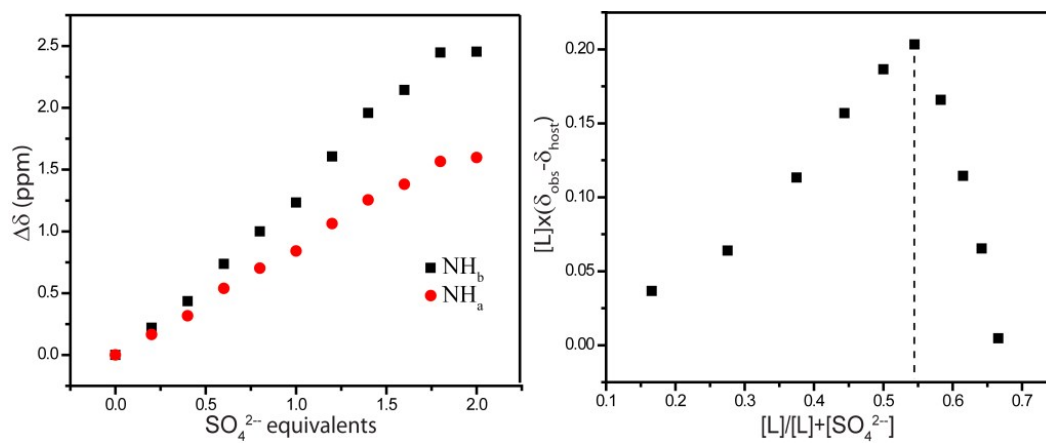


Figure S17: Change in chemical shift of $-\text{NH}$ resonances of **L** (10 mM) with increasing concentration of standard SO_4^{2-} solution (50 mM) in DMSO-d_6 at 298 K and the corresponding Job's plot.

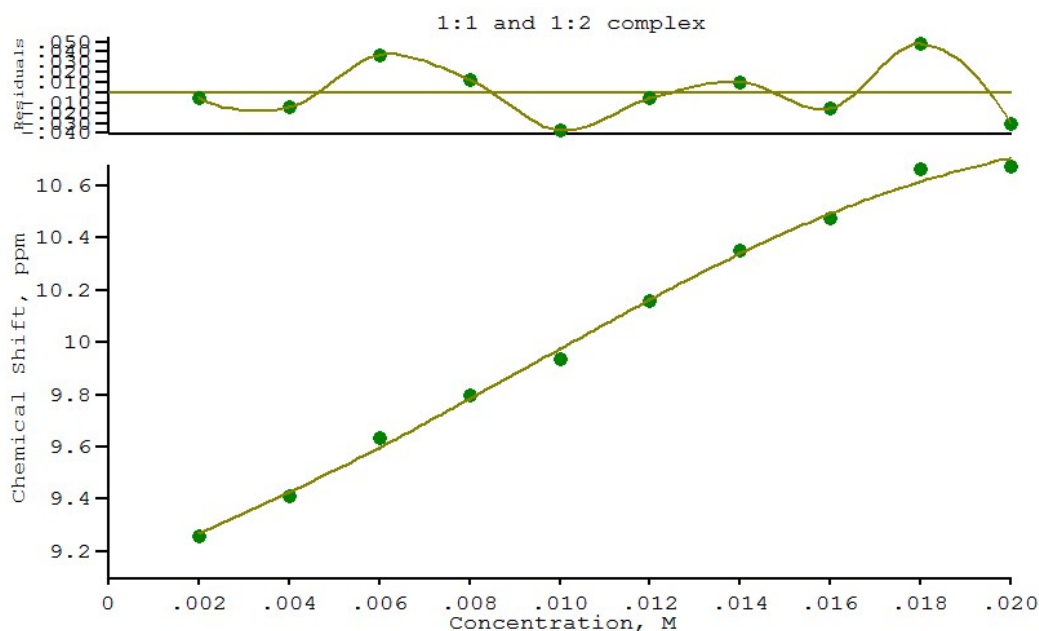


Figure S18: Change in chemical shift of $-\text{NH}_a$ resonances of **L** (10 mM) with increasing concentration of standard SO_4^{2-} solution (50 mM) in DMSO-d_6

Calculations by WinEQNMR2 Version 2.00 by Michael J. Hynes
 Program run at 10:23:55 on 08/09/2017

1:1 and 1:2 complex

Equilibrium constants are log10 values

NO. A PARAMETER DELTA ERROR CONDITION DESCRIPTION

1 1 2.44173E+00 3.200E-02 2.381E+00 7.590E+02 K11
 2 1 5.04534E+00 3.600E-02 6.543E-01 3.369E+02 K12
 3 1 9.12413E+00 1.000E-02 6.688E-02 7.405E+00 Free Ligand
 4 1 1.00087E+01 1.000E-02 1.148E+00 5.855E+02 complex11
 5 1 1.10217E+01 1.000E-02 9.252E-01 1.242E+03 complex12

ORMS ERROR = 3.68E-02 MAX ERROR = 4.79E-02 AT OBS.NO. 9

RESIDUALS SQUARED = 6.76E-03

RFACTOR = 0.2587 PERCENT

NO.	A	EXPT.	DEL	CALC.	DEL	RESIDUAL	% DEV	WEIGHT	SO42-	L	pH
1	1	9.2610E+00	9.2666E+00	-5.6362E-03	-6.0860E-02	1.0000E+00	2.0000E-03	9.6000E-03	0.0000E+00		
2	1	9.4130E+00	9.4274E+00	-1.4425E-02	-1.5325E-01	1.0000E+00	4.0000E-03	9.2000E-03	0.0000E+00		
3	1	9.6340E+00	9.5971E+00	3.6897E-02	3.8298E-01	1.0000E+00	6.0000E-03	8.9000E-03	0.0000E+00		
4	1	9.7980E+00	9.7851E+00	1.2913E-02	1.3179E-01	1.0000E+00	8.0000E-03	8.4000E-03	0.0000E+00		
5	1	9.9370E+00	9.9743E+00	-3.7262E-02	-3.7498E-01	1.0000E+00	1.0000E-02	8.0000E-03	0.0000E+00		
6	1	1.0158E+01	1.0164E+01	-5.5628E-03	-5.4763E-02	1.0000E+00	1.2000E-02	7.6000E-03	0.0000E+00		
7	1	1.0350E+01	1.0340E+01	1.0447E-02	1.0093E-01	1.0000E+00	1.4000E-02	7.2000E-03	0.0000E+00		
8	1	1.0477E+01	1.0492E+01	-1.5385E-02	-1.4684E-01	1.0000E+00	1.6000E-02	6.8000E-03	0.0000E+00		
9	1	1.0662E+01	1.0614E+01	4.7938E-02	4.4962E-01	1.0000E+00	1.8000E-02	6.4000E-03	0.0000E+00		
10	1	1.0674E+01	1.0704E+01	-3.0411E-02	-2.8491E-01	1.0000E+00	2.0000E-02	6.0000E-03	0.0000E+00		

TOLERANCE ON SUM OF SQUARES 0.0100

TOLERANCE ON EIGEN VALUES 0.0001

CONVERGANCE AFTER 19 ITERATIONS

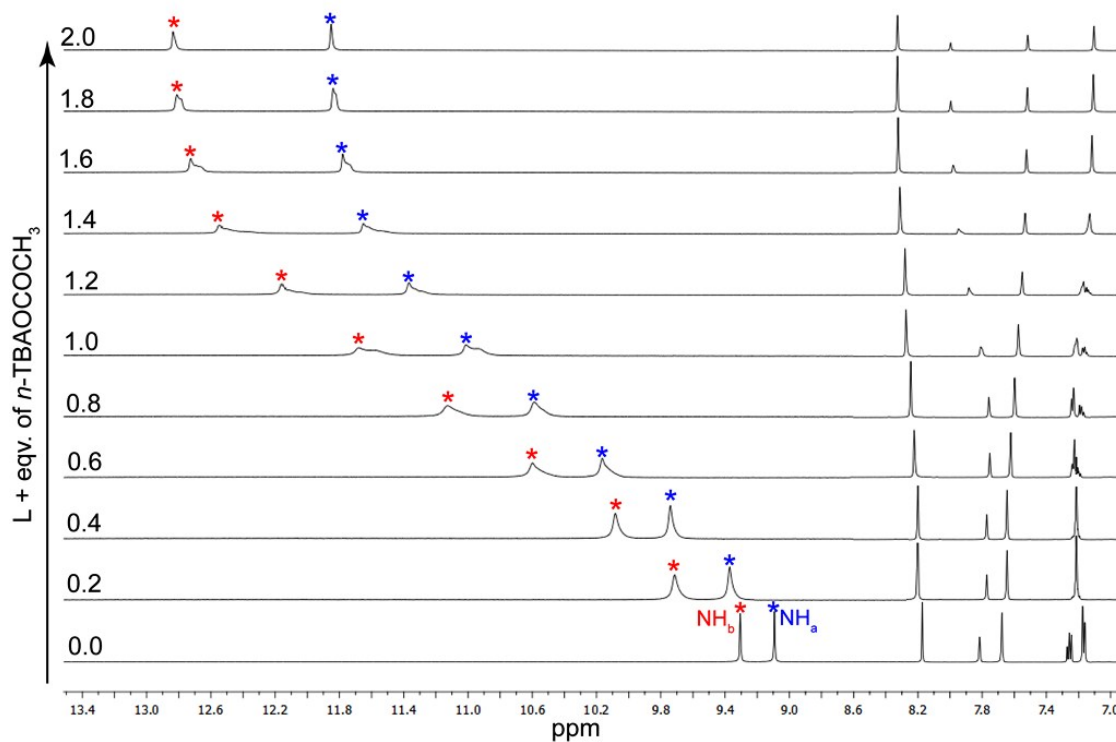


Figure S19: Expanded partial ^1H NMR spectra of **L** upon titration with *n*-TBAOCOCH₃ in DMSO-*d*₆.

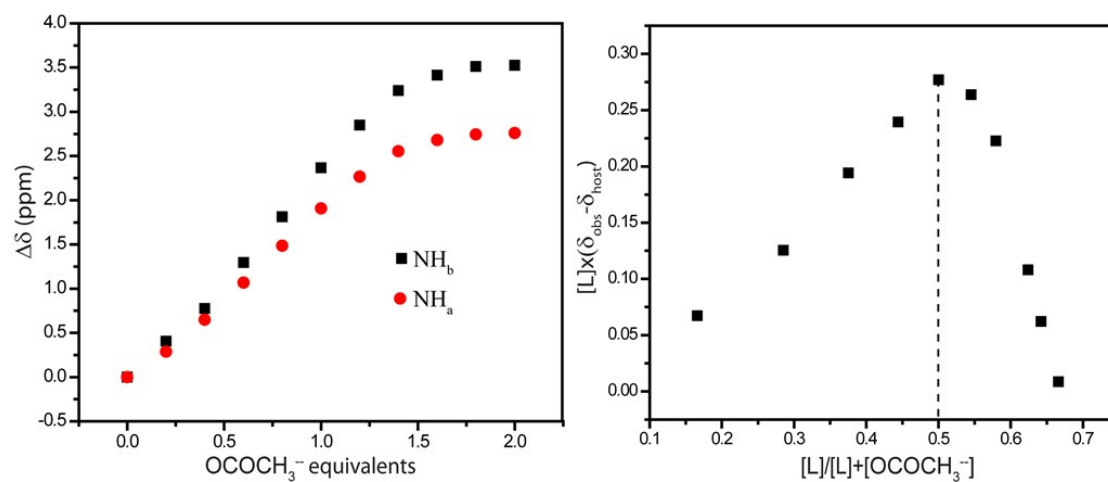


Figure S20: Change in chemical shift of $-\text{NH}$ resonances of **L** (10 mM) with increasing conc. of standard OCOCH₃⁻ solution (50 mM) in DMSO-*d*₆ at 298 K and the corresponding Job's plot.

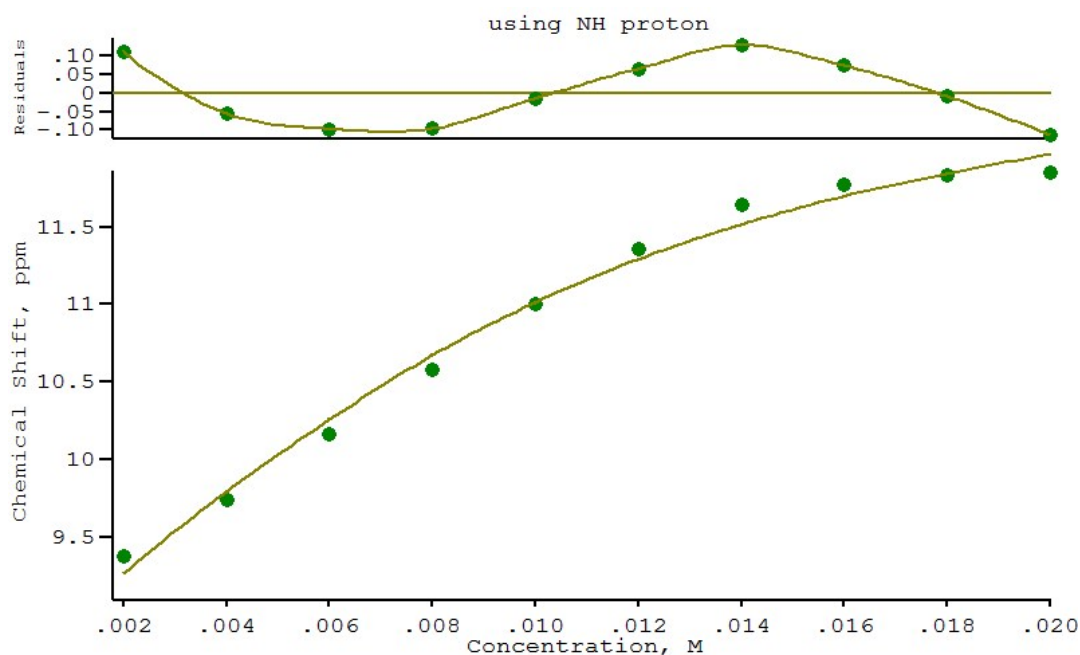


Figure S21: Change in chemical shift of -NH_a resonances of **L** (10 mM) with increasing concentration of standard OCOCH_3^- solution (50 mM) in DMSO-d_6

Calculations by WinEQNMR2 Version 2.00 by Michael J. Hynes
 Program run at 02:14:10 on 08/09/2017

using NH proton

Equilibrium constants are log10 values

NO.	A	PARAMETER	DELTA	ERROR	CONDITION	DESCRIPTION
1	1	2.30927E+00	1.000E-02	1.603E-01	6.194E+01	K1
2	1	8.70554E+00	9.090E-02	1.157E-01	3.463E+00	free ligand
3	1	1.30001E+01	1.186E-01	4.121E-01	4.987E+01	complex

ORMS ERROR = 1.03E-01 MAX ERROR = 1.30E-01 AT OBS.NO. 7
 RESIDUALS SQUARED = 7.38E-02
 RFACTOR = 0.7834 PERCENT

NO.	A	EXPT.	DEL	CALC.	DEL	RESIDUAL	% DEV	WEIGHT	OAC-	L	pH
1	1	9.3790E+00	9.2686E+00	1.1045E-01	1.1776E+00	1.0000E+00	2.0000E-03	9.6000E-03	0.0000E+00		
2	1	9.7400E+00	9.7942E+00	-5.4196E-02	-5.5643E-01	1.0000E+00	4.0000E-03	9.2000E-03	0.0000E+00		
3	1	1.0161E+01	1.0258E+01	-9.7404E-02	-9.5860E-01	1.0000E+00	6.0000E-03	8.9000E-03	0.0000E+00		
4	1	1.0577E+01	1.0673E+01	-9.5893E-02	-9.0662E-01	1.0000E+00	8.0000E-03	8.4000E-03	0.0000E+00		
5	1	1.1001E+01	1.1015E+01	-1.3565E-02	-1.2331E-01	1.0000E+00	1.0000E-02	8.0000E-03	0.0000E+00		
6	1	1.1359E+01	1.1292E+01	6.6730E-02	5.8746E-01	1.0000E+00	1.2000E-02	7.6000E-03	0.0000E+00		
7	1	1.1647E+01	1.1517E+01	1.3018E-01	1.1177E+00	1.0000E+00	1.4000E-02	7.2000E-03	0.0000E+00		
8	1	1.1773E+01	1.1698E+01	7.4896E-02	6.3617E-01	1.0000E+00	1.6000E-02	6.8000E-03	0.0000E+00		
9	1	1.1837E+01	1.1845E+01	-8.3256E-03	-7.0335E-02	1.0000E+00	1.8000E-02	6.4000E-03	0.0000E+00		
10	1	1.1853E+01	1.1966E+01	-1.1287E-01	-9.5227E-01	1.0000E+00	2.0000E-02	6.0000E-03	0.0000E+00		

TOLERANCE ON SUM OF SQUARES 0.0100
 TOLERANCE ON EIGEN VALUES 0.0001
 CONVERGANCE AFTER 17 ITERATIONS

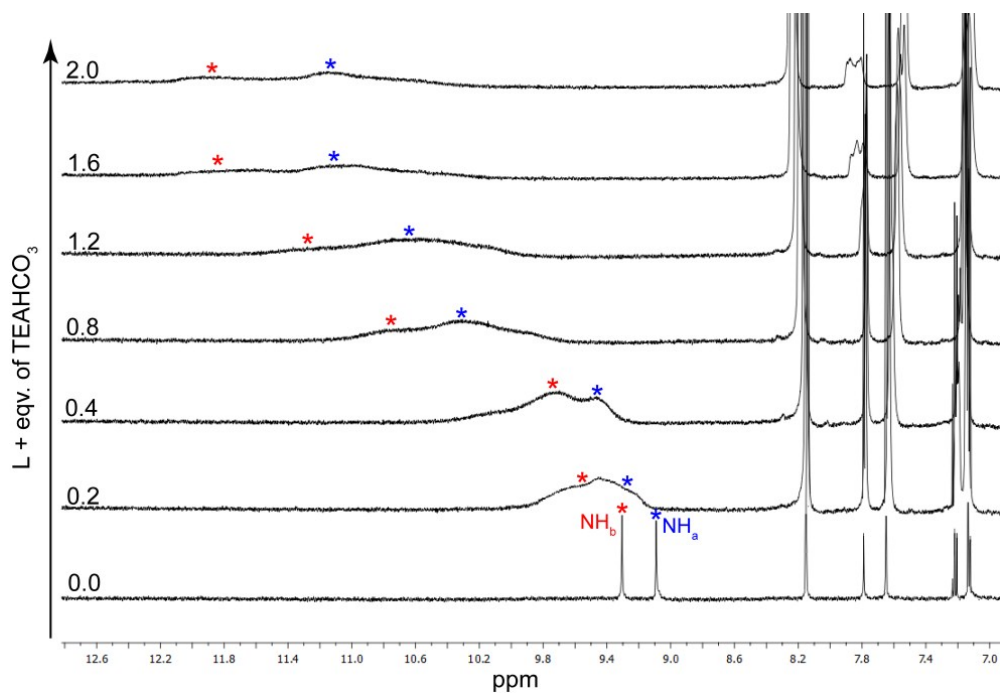


Figure S22: Expanded partial ^1H NMR spectra of **L** upon titration with TEAHCO_3 in DMSO-d_6 showing severe broadening of urea $-\text{NH}$ peaks on gradual anion addition.

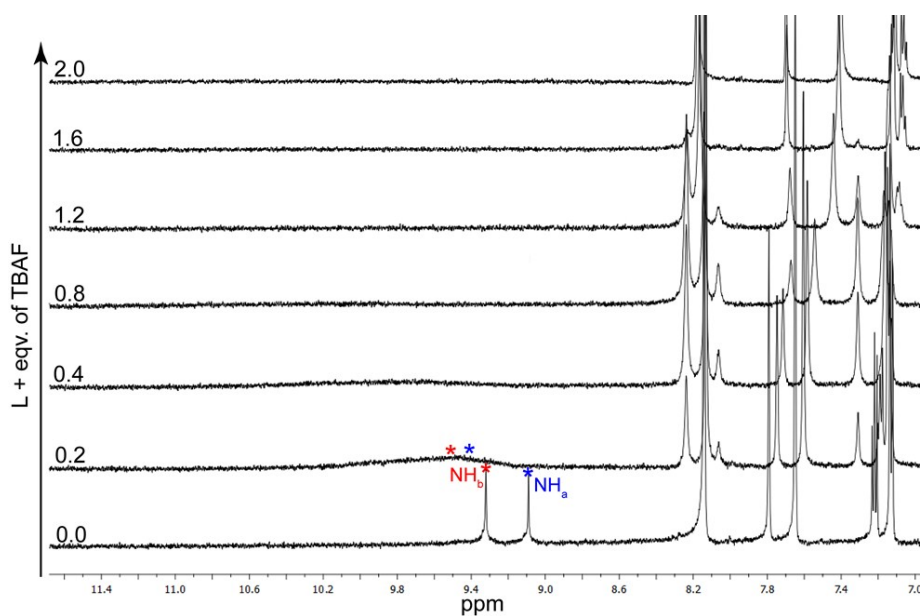


Figure S23: Expanded partial ^1H NMR spectra of **L** upon titration with *n*-TBAF in DMSO-d_6 displaying disappearance of urea $-\text{NH}$ peaks followed by severe broadening may be due to deprotonation.

Table S1. Hydrogen bonding distances (Å) and Bond angles (°) in free ligand and its complexes **1**, **2**, **3** and **4**):

Complex	D-H...A	$d(D\cdots H)/\text{Å}$	$d(H\cdots A)/\text{Å}$	$d(D\cdots A)/\text{Å}$	$\angle D-H\cdots A/^\circ$	Symmetry codes
L.DMF	N1-H1N...O5	0.86	2.14	2.940(5)	156	1-x,-1/2+y,1/2-z
	N2-H2N...O5	0.86	2.03	2.843(5)	157	1-x,-1/2+y,1/2-z
	N5-H5N...O6	0.86	2.05	2.863(6)	158	1-x,1-y,1-z
	N6-H6N...O6	0.86	2.13	2.932(6)	156	1-x,1-y,1-z
	N7-H7N...O7	0.86	2.00	2.821(6)	161	x,y,z
	N8-H8N...O8	0.86	2.12	2.880(6)	146	x,y,z
L.DMSO	N1-H1N...O4	0.86	2.07	2.883(6)	158	1-x,-y,1-z
	N2-H2N...O4	0.86	2.10	2.908(5)	157	1-x,-y,1-z
1	N1-H1N...O10	0.86	1.97	2.817(7)	168	-1+x,y,z
	N2-H2N...O9	0.86	1.99	2.805(6)	157	-1+x,y,z
	N3-H3N...O8	0.86	2.01	2.843(6)	162	1-x,1/2+y,1/2-z
	N4-H4N...O7	0.86	1.93	2.750(6)	159	1-x,1/2+y,1/2-z
	N5-H5N...O12	0.86	2.26	3.082(8)	160	x,y,z
	N5-H5N...O13		2.57	3.277(6)	140	x,y,z
	N6-H6N...O13	0.86	2.00	2.831(6)	163	x,y,z
	N7-H7N...O8	0.86	2.05	2.842(6)	153	-1+x,y,z
	N8-H8N...O9	0.86	1.87	2.729(6)	175	-1+x,y,z
	N9-H9N...O14	0.86	1.93	2.769(7)	167	1-x,-1/2+y,1/2-z
	N10-H10N...O12	0.86	2.27	3.113(8)	166	1-x,-1/2+y,1/2-z
	N11-H11N...O11	0.86	1.99	2.845(6)	171	x,y,z
	N12-H12N...O13	0.86	2.01	2.841(6)	162	x,y,z
	C114-H24C...O4	0.97	2.39	3.343(12)	166	x,y,z
	C121-H31C...O6	0.97	2.35	3.311(8)	171	1-x,1/2+y,1/2-z
	C125-H35D...O10	0.97	2.40	3.300(7)	154	x,y,z
	C73-H73B...F9	0.97	2.51	3.327(13)	142	1-x,1-y,1-z
	C87-H87A...O16	0.97	2.13	3.01(6)	151	x,y,z
	C93-H93B...O3	0.97	2.44	3.381(12)	163	x,y,z
	C97-H97A...F5	0.97	2.53	3.460(13)	160	-x,1-y,1-z
C98-H98B...O2	0.97	2.39	3.298(10)	156	x,y,z	
2	N1-H1N...O3	0.86	1.89	2.724(5)	165	x,y,z
	N2-H2N...O4	0.86	1.95	2.802(5)	172	x,y,z
	N3-H3N...O7	0.86	1.92	2.777(5)	173	x,y,z
	N4-H4N...O6	0.86	1.92	2.767(5)	167	x,y,z
	O5-H5O...O7	0.99	1.63	2.614(7)	174	-x,1/2+y,1/2-z
	O8-H8O...O4	1.00	1.70	2.611(5)	149	-x,-1/2+y,1/2-z
	C26-H26B...O5	0.97	2.59	3.408(9)	143	x,3/2-y,-1/2+z
	C33-H33B...O2	0.97	2.40	3.336(8)	162	x,y,z
	C37-H37B...O3	0.97	2.54	3.425(7)	153	x,3/2-y,-1/2+z
	C38-H38B...O2	0.97	2.45	3.372(7)	159	x,y,z
	C49-H49A...O6	0.97	2.59	3.436(7)	145	x,1/2-y,1/2+z
	C50-H50A...O1	0.97	2.58	3.490(7)	156	x,y,z
	C53-H53A...O1	0.97	2.43	3.368(7)	163	x,y,z
	3	N1-H1N...O3	0.86	2.01	2.859(8)	169
N2-H2N...O4		0.86	1.94	2.784(8)	168	1-x,-1/2+y,-z
N3-H3N...O5		0.86	2.17	2.981(7)	157	-1+x,y,z
N4-H4N...O5		0.86	2.00	2.832(8)	162	-1+x,y,z
C29-H29A...O2		0.97	2.58	3.495(15)	158	x,y,z
C36-H36A...F1		0.96	2.50	3.31(2)	142	-1+x,1+y,z
4	N1-H1N...O3A	0.86	2.24	3.059(9)	158	-x,y,1/2-z
	N1-H1N...O3B	0.86	2.37	3.173(14)	155	-x,y,1/2-z
	N2-H2N...O3A	0.86	2.45	3.231(9)	152	-x,y,1/2-z
	N2-H2N...O3B	0.86	2.18	3.023(14)	165	-x,y,1/2-z
	N3-H3N...C11	0.86	2.40	3.210(3)	158	x,y,z
	N4-H4N...C11	0.86	2.31	3.119(3)	157	x,y,z

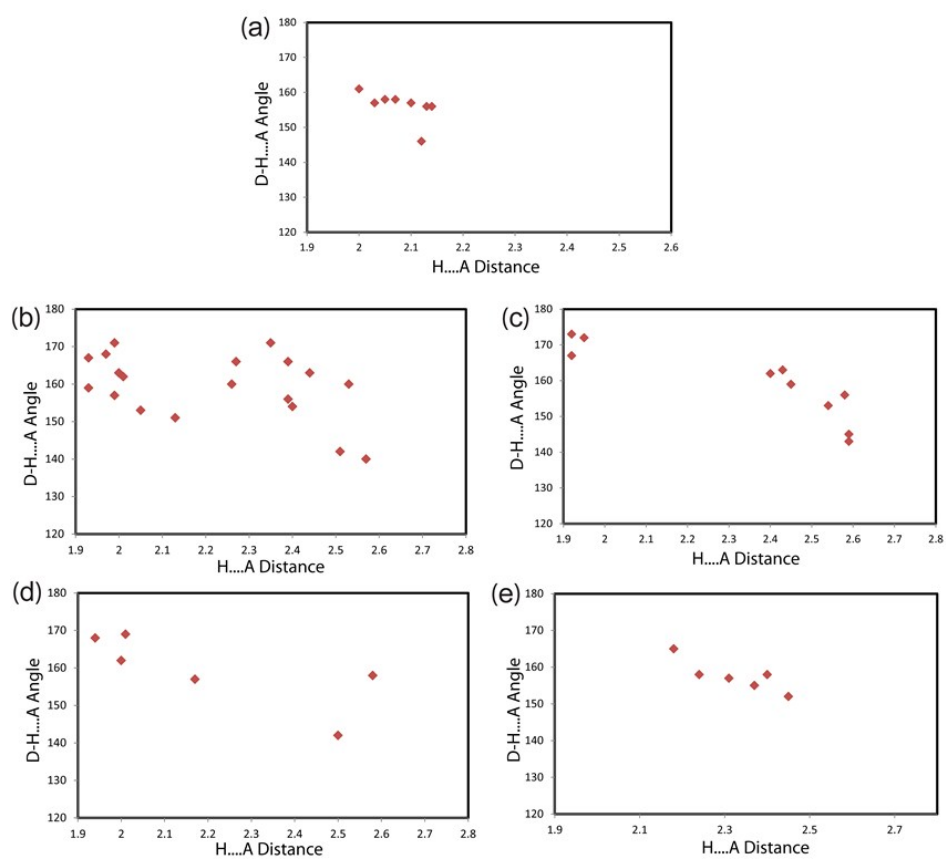
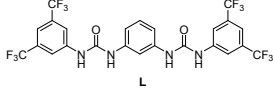
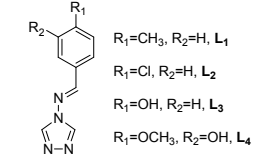
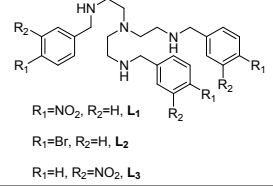
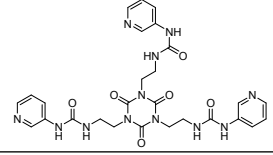
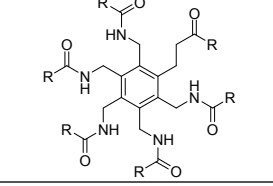
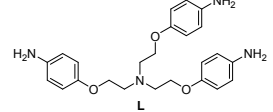


Figure S24. The scatter plot of N-H...A angle vs. H...A distance of the hydrogen bonds in (a) free receptor **L** and in the complexes (b) complex **1**, (c) complex **2**, (d) complex **3** and (e) complex **4**.

Table S2. Comparison of some recently reported anion-water clusters and CO₂ fixation with the present work.

Sl. No	Reference	Host-guest complex	Receptor/Ligand	Hydrated-halide recognition	Hydrated-oxyanion recognition	Aerial CO ₂ fixation	Conclusion/observation from result
1	Present work	Neutral		Acyclic (Cl ⁻) ₂ (H ₂ O) ₂	a) asymmetric (SO ₄) ₂ (H ₂ O) ₂ b) Polymeric [(OCOCH ₃)(H ₂ O)] _n	F ⁻ induced (HCO ₃) ₂ dimer	Consistent and regular anion binding mode of semi-circular receptor architecture in all anion complexes are heavily influenced by the terminal aromatic <i>meta</i> -disubstitution of receptor
2	Y-H. Luo, J-W. Wang , Y-J. Li , C. Chen , P.-J. An, S-L. Wang , C-Q. You and B-W. Sun, <i>CrystEngComm</i> , 2017, 19 , 3362	Protonated		—	a) [HSO ₄ ⁻ ·H ₂ O] _n or [SO ₄ ²⁻ ·H ₂ O] _n with HL ₁ ⁺ , HL ₂ ⁺ and HL ₄ ⁺ b) [HL ₃] ⁺ [NO ₃] ⁻ ·H ₂ O	—	Approach for aqueous/sea- water sulphate separation
3	U. Manna, B. Nayak, M. N. Hoque and G. Das, <i>CrystEngComm</i> , 2016, 18 , 5036	Protonated		—	a) [(L ₁ H ₃) ₂ (SO ₄) ₃ (H ₂ O) ₈]·3DMF b) [(L ₂ H ₃) ₂ (SO ₄) ₃ (H ₂ O) ₈]·4DMF	—	Consequence of halide and oxyanion size on capsular/non-capsular assembly formation of positional isomeric tripodal polyamine receptors
4	R. Dutta, B. Akhuli and P. Ghosh <i>Dalton Trans.</i> , 2015, 44 , 15075	Neutral		—	[(SO ₄) ₄ (H ₂ O) ₁₂] ⁸⁻	—	Recognition of hydrated sulfate cluster [(SO ₄) ₄ (H ₂ O) ₁₂] ⁸⁻ in a self-assembled metal-organic coordination polymer
5	S.Chakraborty, M. Arunachalam, R. Dutta and P. Ghosh, <i>RSC Adv.</i> , 2015, 5 , 48060	Neutral		[(L ₄).(Cl) ₂ .(H ₂ O) ₂ .(TBA) ₂]	—	—	Binding of anions/hydrated anions of different dimensionalities to the hexa-amide receptors with different structural arrangements
6	M. N. Hoque and G. Das, <i>CrystEngComm</i> , 2014, 16 , 4447	Protonated		a) [LH ₄ ·4F·5H ₂ O] b) [2LH ₄ ·8Cl·5H ₂ O] c) [LH ₄ ·4Br·5H ₂ O] d) [4LH ₄ ·16I·7H ₂ O]	—	—	Capsular and non-capsular assembly of cationic tripodal receptor with hydrophilic halide-water cluster

7	A. Pati, J. Athilakshmi, V. Ramkumar and D. K. Chand, <i>CrystEngComm</i> , 2014, 16 , 6827	Neutral		$\{[(\text{H}_2\text{O})_{12}(\text{Cl})]^{1-}\}_n$ cluster of L_1 and L_2	—	—	Hydrophobic cavity induced reductive encapsulation using Hg(II) and an octaaza cryptand offering a new type of polydodecameric water-chloride cluster
8	M. N. Hoque and G. Das, <i>Cryst. Growth Des.</i> , 2014, 14 , 2962	Protonated		—	a) $[\text{LH}_4 \cdot 4\text{H}_2\text{PO}_4 \cdot \text{H}_2\text{O}]$ b) $[2\text{LH}_4 \cdot 9\text{ClO}_4 \cdot \text{Na} \cdot 6\text{H}_2\text{O}]$ c) $[\text{LH}_4 \cdot 2\text{HSO}_4 \cdot \text{SO}_4]$ d) $[\text{LH}_4 \cdot 2\text{SO}_4 \cdot \text{H}_2\text{O}]$ e) $[\text{LH}_4 \cdot 4\text{NO}_3 \cdot \text{H}_2\text{O}]$	—	Solid-state characterization of anion and anion-water clusters based on oxyanions
9	R. Custelcean, N. J. Williams, C. A. Seipp, A. S. Ivanov and S. Vyacheslav <i>Chem. Eur. J.</i> 2016, 22 , 1997	Protonated		—	$[(\text{SO}_4)_2(\text{H}_2\text{O})_4]^{4-}$	—	Approach to aqueous sulfate separation by selective crystallization with an imine-linked bis-guanidinium ligand
10	M. N. Hoque, U. Manna, G. Das, <i>Polyhedron</i> , 2016, 119 , 307	Protonated		$[^2\text{LH}_2 \cdot 2\text{I} \cdot 3\text{H}_2\text{O}]$	a) $[^3\text{LH}_2 \cdot \text{HPO}_4 \cdot \text{H}_2\text{O}]$ b) $[^3\text{LH}_2 \cdot 2\text{ClO}_4 \cdot \text{H}_2\text{O}]$ c) $[^4\text{LH}_2 \cdot 2\text{NO}_3 \cdot 3\text{H}_2\text{O}]$ d) $[^4\text{LH}_2 \cdot \text{HPO}_4 \cdot 3\text{H}_2\text{O}]$ e) $[^4\text{LH}_2 \cdot 2\text{ClO}_4 \cdot \text{H}_2\text{O}]$	—	Solid state recognition of anions in their various hydrated states by H-bond rich isomeric pyridine-urea receptor
11	U. Manna, R. Chutia, and G. Das, <i>Cryst. Growth Des.</i> 2016, 16 , 2893	Neutral		$[n\text{-TBA}\{\text{L}_1(\text{F})(\text{H}_2\text{O})\}]$	$4(n\text{-TBA})[3\text{L}_2\{(\text{SO}_4)(\text{H}_2\text{O})_3\text{-}(\text{SO}_4)\}]$	—	Positional isomeric bis-urea receptors unveil as efficient hosts toward anion water cluster/adducts
12	I. Ravikumar and P. Ghosh, <i>Chem. Commun.</i> , 2010, 46 , 1082	Neutral		—	—	OH ⁻ induced CO ₃ ²⁻ encapsulation	Fixation of environmental carbon dioxide in the form of carbonate in a molecular capsule of an easily synthesized urea based receptor
13	R. Chutia and G. Das, <i>Dalton Trans.</i> , 2014, 43 , 15628	Neutral		—	—	F ⁻ induced (HCO ₃) ₂ dimer	Combined act of hydrogen and halogen bonding that prompted the CO ₂ uptake from a fluoride
14	R. Dutta, S. Chakraborty, P. Bose and P. Ghosh, <i>EJC.</i> , 2014, 2014 , 4134	Neutral		—	—	OH ⁻ induced CO ₃ ²⁻ encapsulation	Efficient encapsulation of CO ₃ ²⁻ ions through the fixation of aerial CO ₂ , extractant for Chromate, sulfate and thiosulfate
15	U. Manna, S. Kayal, S. Samanta and G. Das, <i>Dalton Trans.</i> , 2017, 46 , 10374.	Neutral		—	$[(n\text{-TBA})_4\{(\text{L})_4(\text{CO}_3)_2(\text{H}_2\text{O})_2\}]$	OH ⁻ induced {CO ₃ ²⁻ -(H ₂ O) ₂ -CO ₃ ²⁻ } entrapment	Anion recognition is more affected by the size and dimension of the anions rather than the terminal aromatic substituent effect